J. Fluid Mech. (1991), *vol.* 232, *pp.* 403–413
Printed in Great Britain

Testing continuum descriptions of low-Mach-number shock structures

By GERALD C. PHAM-VAN-DIEP, DANIEL A. ERWIN† AND E. PHILLIP MUNTZ

University of Southern California, Department of Aerospace Engineering, Los Angeles, CA 90089-1191, USA

(Received 20 September 1990 and in revised form 23 March 1991)

Numerical experiments have been performed on normal shock waves with Monte Carlo Direct Simulations (MCDS's) to investigate the validity of continuum theories at very low Mach numbers. Results from the Navier–Stokes and the Burnett equations are compared to MCDS's for both hard-sphere and Maxwell gases. It is found that the maximum-slope shock thicknesses are described equally well (within the MCDS computational scatter) by either of the continuum formulations for Mach numbers smaller than about 1.2. For Mach numbers greater than 1.2, the Burnett predictions are more accurate than the Navier–Stokes results. Temperature–density profile separations are best described by the Burnett equations for Mach numbers greater than about 1.3. At lower Mach numbers the MCDS scatter is too great to differentiate between the two continuum theories. For all Mach numbers above one, the shock shapes are more accurately described by the Burnett equations.

1. Introduction

The validity of various continuum descriptions of normal shock structure has been addressed before in a large number of theoretical and experimental investigations (Liepmann, Narasimha & Chahine 1962; Elliott 1975; Fiszdon, Herczyński & Walenta 1974). Two publications (Pham-Van-Diep, Erwin & Muntz 1989; Erwin, Pham-Vam-Diep & Muntz 1991) by the authors of the present paper have established a detailed experimental validation of Bird's (1976) Monte Carlo Direct Simulation (MCDS) computational method. In these two papers it was shown that if appropriately detailed physical inputs are used, MCDS's can predict with high accuracy not only macroscopic property profiles, but also the molecular motion throughout the interior of normal shock waves.

In this paper, numerical experiments are used to investigate normal shock wave behaviour at low shock Mach numbers. The experimental study of these shock waves is difficult because there are only small changes in the flow properties over comparatively large distances. This leads to experimental errors connected with instrumentation accuracy as well as upstream and downstream boundary conditions. Similar issues confront the MCDS's; however, with long runs to accumulate statistics and with proper treatment of the boundary conditions (see below) these difficulties can, for the most part, be negated.

In order to study low-Mach-number shock waves, MCDS's have been made for several real and fictitious gases. The MCDS's are treated as if they were experiments

† To whom correspondence should be addressed.

and compared to shock transition properties obtained from the Navier–Stokes and Burnett equations. Of particular interest here is the limiting behaviour at low shock Mach numbers, where definitive experimental studies have not been possible.

2. Background

2.1. *Shock profile nomenclature*

For the purposes of this paper the shock profile characteristics defined in figure 1 are of importance. All are suitable for evaluation from experimental (or computational) data. The maximum-slope shock thickness δ_s is a traditional measure of the characteristic size of the shock transition. A useful single-parameter indicator of shock shape is Q (Schmidt 1969). Distances are frequently non-dimensionalized by the free-stream mean free path calculated using the Chapman–Enskog first approximation to the mean free path for hard-sphere monatomic gases (Chapman & Cowling 1952):

$$\lambda_1 = \frac{16}{5}\left(\frac{5}{6\pi}\right)^{\frac{1}{2}}\frac{\eta_1}{\rho_1 a_1}, \tag{1}$$

where a_1, η_1 and ρ_1, respectively, are the sound speed, viscosity and density in the upstream flow. The separation between the temperature and density profiles is given by $\Delta_{T\rho}$ at $\tilde{n}$ and $\tilde{T} = 0.5$. The non-dimensional quantities $\tilde{n}$ and $\tilde{T}$ are defined in figure 1 and are convenient for discussing shock structure.

2.2. *Continuum theories and MCDS's*

It is generally accepted (Liepmann *et al.* 1962; Fiszdon *et al.* 1974) that the Navier–Stokes equations should describe shock transitions at low Mach numbers. However, according to another viewpoint (Elliott 1975), the Navier–Stokes equations are inadequate even at extremely low Mach numbers. This work uses the shock wave solutions for the Navier–Stokes equations given by Gilbarg & Paolucci (1953) and Lumpkin & Chapman (1991); those for the Burnett equations are taken from Simon & Foch (1977), Talbot & Sherman (1960), and Lumpkin & Chapman (1991).

2.3. *Computational considerations*

The work reported here employed a one-dimensional MCDS code originally written by Bird (1989) and subsequently modified by the authors (Pham-Van-Diep *et al.* 1989; Erwin *et al.* 1991). The code differed from earlier versions chiefly in the calculation of the number of collisions per time step, formerly done with the time counter method but now with the 'no time counter' method, wherein the number of collisions is obtained directly based on the maximum biatomic collision rate in each cell. In this code, the shock develops normal to the x-axis which is divided into a grid of 100 or more cells, each made of 10 sub-cells, corresponding to an interval of a few centimeters containing the shock. The ratio of simulated to real atoms is chosen such that there are approximately 100 simulated atoms per cell. The grid is non-uniform, the cell size decreasing in the downstream direction so that the number of simulated particles per cell is almost constant.

Inputs to the program are the free-stream ($x \ll 0$) conditions and the shock Mach number M. The free-stream conditions are used as the boundary conditions at the upstream grid edge: entering atoms are sampled from an equilibrium (drifting Maxwellian) distribution, while the downstream boundary is a surface of specular reflection in motion at the Rankine–Hugoniot velocity. This downstream boundary

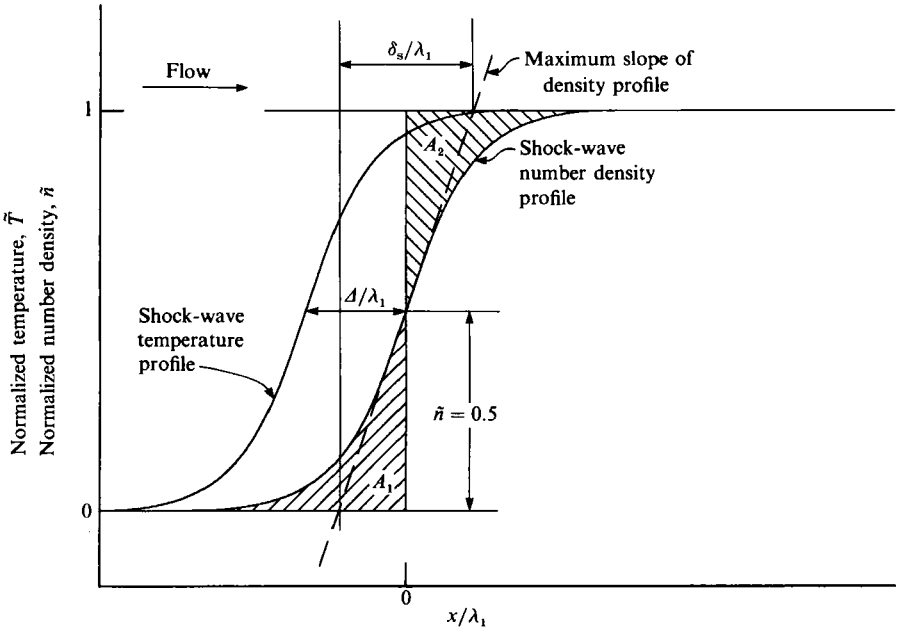

FIGURE 1. Nomenclature. The flow direction is left to right. The temperature profile and the density profile are both normalized to zero upstream and unity downstream of the shock [$\tilde{T} \equiv (T-T_1)/(T_2-T_1)$, $\tilde{n} \equiv (n-n_1)/(n_2-n_1)$]. (The subscript 1 denotes conditions ahead of the shock (to the left), while 2 denotes those downstream of the shock.) The separation between these profiles is the temperature–density shift Δ, measured at $\tilde{n} = 0.5$. The dashed line is the line tangent to the density profile at the maximum slope; the horizontal distance between its intersections with the lines $\tilde{n} = 0$ and $\tilde{n} = 1$ is the maximum-slope shock thickness. The ratio of the shaded areas A_1 and A_2 is the shape factor $Q \equiv A_1/A_2$.

condition was introduced by Bird (1989). He pointed out that the more usual use of an equilibrium downstream boundary, in the same manner as the upstream one, produces small disturbances at the boundary which are of the same order as the shock-related changes for low M ($\lesssim 1.5$) and therefore corrupt the solutions. The specular-reflection boundary condition removes this problem.

The computation of low-M shock properties by MCDS requires some care in choosing the correct input conditions. The shock waves are very thick in terms of upstream mean free paths. Thus, in order to maintain the size of computational cells at a fraction of a mean free path, significantly more cells are required in the computation than at higher M. Moreover, at low M the computations have to proceed for a longer-than-normal time to reduce statistical scatter in the results because of the small changes in the flow properties across the shock waves. A tabulation of the computational parameters for the Mach numbers used in the paper is presented in table 1. The table presents for each simulation the Mach number M, the temperature–viscosity exponent s (see below), the number of cells N_C, the number of statistical samples N_S, and the size W of the computational domain.

The MCDS's were performed using single-precision (32-bit) arithmetic. In the calculation of temperatures from the molecular motion, there is a truncation error of about -1 to -2 K for temperatures in the 100–300 K range. This small error is normally of no practical significance, but is noticeable in determining the shift between temperature and density profiles in very low-M shock waves. The error shifts the temperature profiles slightly downstream relative to their correct positions.

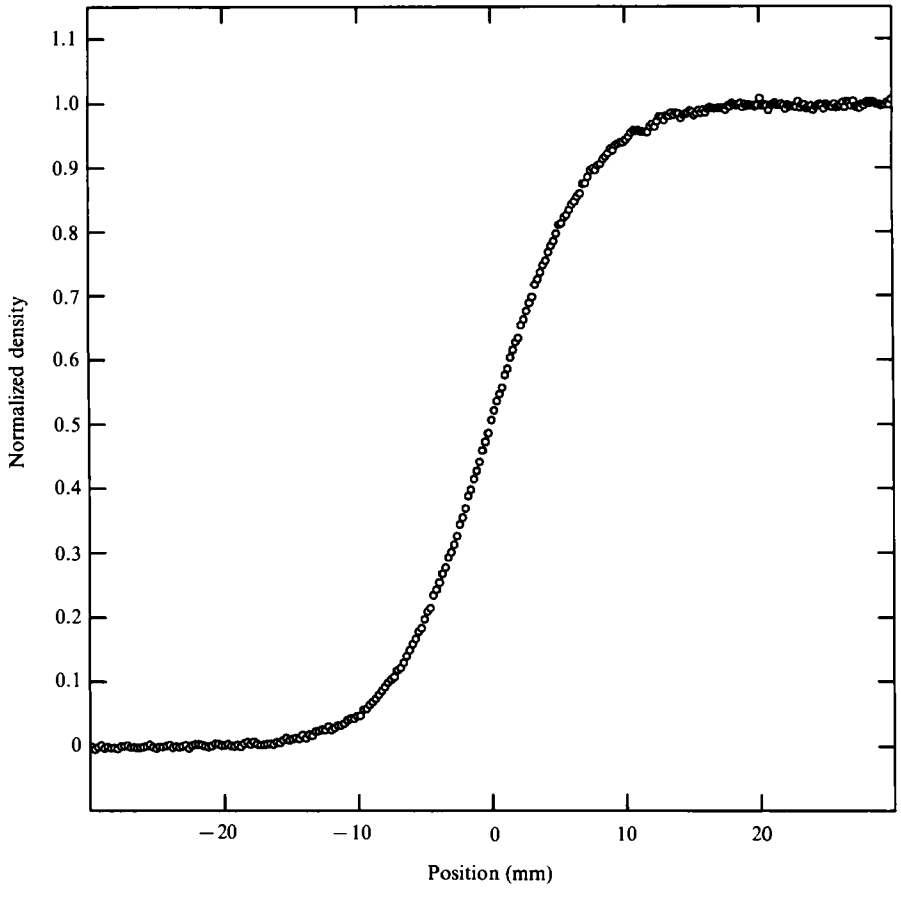

FIGURE 2. Density for each cell after 10000 samples. $M = 1.35$, $s = 0.5$.

M	1.2		1.35		1.5		1.59	
s	1	0.5	1	0.5	1	0.5	1	0.5
N_C	300	300	200	200	100	100	100	—
$N_S \times 10^{-4}$†	2.13	1.11	2.09	1.79	2.68	4.44	2.19	—
W (cm)	10	10	6	6	4	4	4	—

M	1.8		2		2.5	
s	1	0.5	1	0.5	1	0.5
N_C	100	100	100	100	100	100
$N_S \times 10^{-4}$†	4.37	1.04	2.75	1.24	2.17	2.61
W (cm)	4	4	4	4	4	4

† 1 sample ≡ 4 time steps; the time step is variable but $\approx 10^{-7}$ s.

TABLE 1. Computational parameters

Consequently, a correction was made for this shift in the values of Δ_{T_p} reported here. The method for making the correction was verified by comparing its results to the outcome of a MCDS using double-precision arithmetic. Both the corrected single-precision and the double-precision results are shown later in figure 5.

There is a variety of contributors to errors in the calculated shock wave results, although there are no known systematic sources. In many experiments it is most reasonable to infer errors from the results by observing the scatter. In the present case, the best estimate of the importance of random errors is also obtained by looking at the scatter of the results. To aid in this we have placed on the presentations of the results our estimates of the scatter. No estimates of any systematic error are available; note, however, the comparisons to available experimental data made by Erwin *et al.* (1991).

Another indication of reliability is provided by the raw data. A shock wave density profile is shown in figure 2 by plotting as individual points the data from each computational cell. The case shown is after 10000 samples with $s = 0.5$ (see below) and $M = 1.35$. (This is not one of the conditions reviewed in table 1, where it is indicated that for $M = 1.35$, 20000 samples were used; the 20000-sample results exhibited an appropriately reduced scatter compared to figure 2.) Each sample corresponds to four time steps of approximately 10^{-7} s per step. Since data are accumulated for each cell after the initial time required for the flows to become steady, a larger number of samples represents a larger number of measured molecules and thus a lower statistical scatter.

2.4. *Intermolecular potentials*

For the MCDS's presented in this paper, either inverse-power repulsive interatomic potentials ranging from hard spheres to Maxwell molecules, or the Maitland–Smith (Aziz & Chen 1977; Aziz & Nain 1979) potentials for argon and helium, are used. Maitland–Smith potentials have attractive wells and closely mimic actual interatomic potentials. Both types of potentials and their relationship to viscosity as well as the differential scattering cross-sections derived from the potentials are reviewed in detail by Erwin *et al.* (1991). The inverse-power potentials are identified by the corresponding variation of viscosity with temperature,

$$\eta = \eta_{\text{ref}} \left(\frac{T}{T_{\text{ref}}} \right)^s, \tag{2}$$

where $s = 0.5$ for hard spheres and 1 for Maxwell molecules. The power law $\eta \sim T^s$ is consistent with the inverse-power interparticle potential where $\omega = 2/(s-0.5)$:

$$U(r) \sim r^{-\omega}. \tag{3}$$

It is shown by Muntz, Pham-Van-Diep & Erwin (1991) that for the case of low-Mach-number shock waves, differential scattering from inverse-power intermolecular potentials is equivalent to the more usual variable-hard-sphere (VHS) scattering scheme introduced by Bird (1981). The majority of the MCDS calculations mentioned here were done with the VHS scattering technique, with the understanding that this collision scheme yields accurate macroscopic and microscopic properties in normal shocks for the Mach-number range investigated ($M \leqslant 2.5$). Some MCDS's using differential scattering from Maitland–Smith potentials are also presented and are clearly identified.

η_{ref} (kg m^{-1} s^{-1})	186×10^{-7}	186×10^{-7}
d_{ref} (Å)	2.19	2.64
T_{ref} (K)	273	273
s	0.5	1
ω	∞	4
λ_1 (mm)	1.61	1.25

TABLE 2. Values of gas characteristics used in computations involving inverse-power potentials (η_{ref} and d_{ref} are for helium)

2.5. *Lengthscales for presentations of results*

In the original MCDS code, the interaction between atoms is modelled by VHS scattering assuming an inverse-power interatomic potential (Bird 1976). By matching viscosity data in the temperature range of interest, a VHS reference diameter d_{ref} can be determined (Bird 1981):

$$d_{ref} = \left[\frac{15[205-12\omega(2-\omega)]}{16(101-6\omega)}\right]^{\frac{1}{2}} \frac{(mkT_{ref}/\pi)^{\frac{1}{4}}}{[\Gamma(4-\omega)\{2-\omega\}^{\omega}\eta_{ref}]^{\frac{1}{2}}}, \tag{4}$$

where T_{ref}, η_{ref}, m and k are the reference temperature, reference viscosity, mass of the atom and the Boltzmann constant, respectively; ω was defined in (3).

A VHS mean free path was also derived by Bird (1983):

$$\lambda = \frac{(2\eta/15)(7-2\omega)(5-2\omega)}{\rho(2\pi kT/m)^{\frac{1}{2}}}, \tag{5}$$

where ρ is the gas density. Note that the VHS mean free path (Bird 1983) differs from the Chapman–Enskog mean free path (equation (1)) by the factor $(7-2\omega)(5-2\omega)/24$. This difference is important when the mean free path is used for normalization purposes. The values of d_{ref}, reference viscosities and temperatures used for the VHS MCDS's reported here are reproduced in table 2 for reference. Since the MCDS code requires absolute inputs, the helium reference values from table 2 were used for all of the computations involving inverse-power potentials. The free-stream number density was always $n_1 = 2.889 \times 10^{21}$ m^{-3} and the free-stream temperature $T_1 =$ 160 K. Different Mach numbers were generated by varying the free-stream velocities.

3. Results and discussion

MCDS shock thickness (δ_s) computations are compared in figure 3 to Navier–Stokes (Gilbarg & Paolucci 1953) and Burnett (Talbot & Sherman 1960; Lumpkin & Chapman 1991) predictions. The low-Mach-number behaviour of the MCDS results was noted by Erwin *et al.* (1991) and by Bird (1989). Using inverse-power potentials, the MCDS's behave as expected: the shock becomes thicker as s increases, while the sensitivity to s decreases with decreasing Mach number. For reference, MCDS results obtained by employing differential scattering and Maitland–Smith intermolecular potentials are contrasted to the corresponding MCDS (VHS) results in figure 3. For real gases such as argon and helium, as modelled by their Maitland–Smith intermolecular potentials, the shock thicknesses are, as expected, bounded by the MCDS (VHS) predictions for hard-sphere and Maxwell gases. All predictions appear

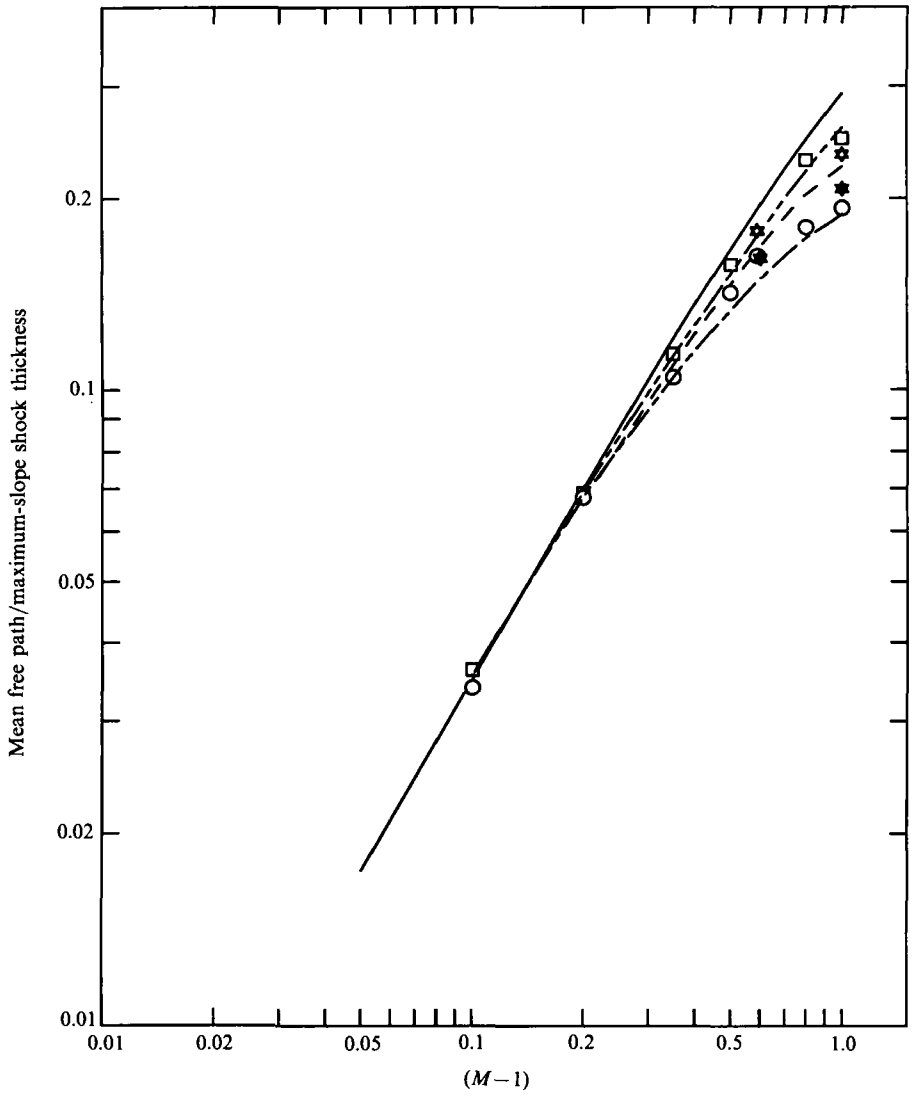

FIGURE 3. Normalized inverse maximum slope shock thickness *vs.* Mach number (MCDS *vs.* various theories). ——, – – – –, Navier–Stokes results ($s = 0.5$ and $s = 1$ respectively) of Gilbarg & Paolucci; — — —, the Burnett result ($s = 1$) of Talbot & Sherman; —·—·—, the Burnett result ($s = 0.5$) of Lumpkin & Chapman. The symbols represent the present results: ✡, Maitland–Smith results for wind-tunnel conditions for helium; ●, Maitland–Smith wind-tunnel results for argon; □, $s = 0.5$; ○, $s = 1$. The MCDS error bars are approximately one symbol height.

to be asymptotic to the Navier–Stokes and Burnett curves at Mach numbers below about 1.2. Thus, for real as well as fictitious gases, the low Mach-number asymptotic behaviour of the shock thicknesses agrees with that of both the Navier–Stokes and Burnett equations.

At Mach numbers greater than 1.2, the shock thicknesses for relatively soft real intermolecular potentials such as argon's follow, but are slightly thinner than, the Burnett thicknesses for $s = 1$, at least up to $M = 2$ as demonstrated in figure 3. It may also be seen that the MCDS shock thicknesses for a Maxwell gas support the Burnett thicknesses for $s = 1$ and are in noticeable disagreement with the Navier–Stokes

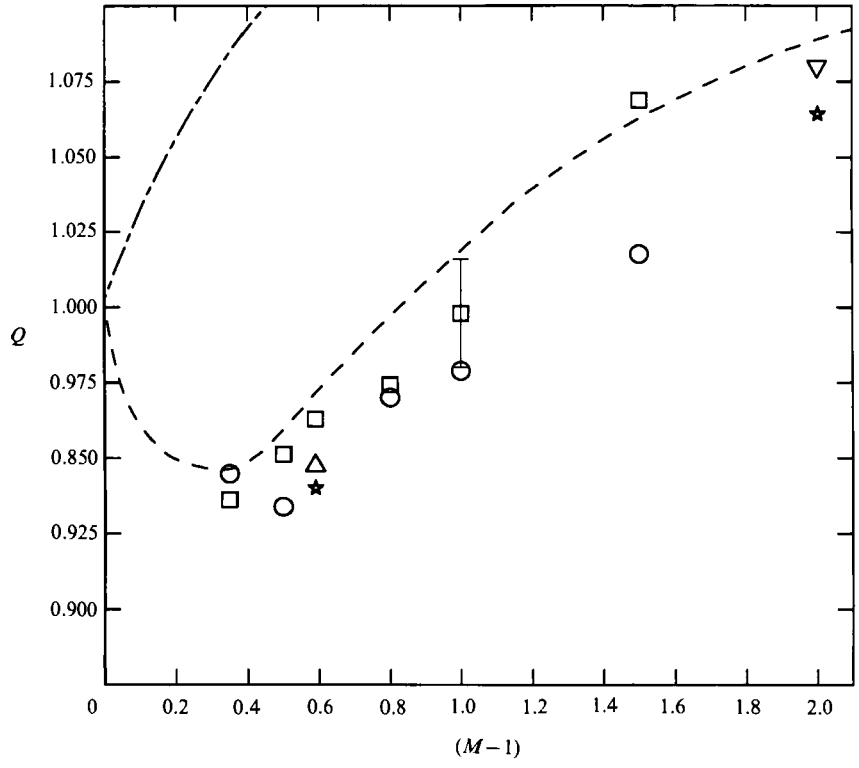

FIGURE 4. Shock shape —·—·-, the Navier–Stokes solution for $s = 1$; – – –, the Burnett solution for $s = 1$, due to Simon & Foch; ▽, the MCDS $s = 0.72$ solution of Fiscko & Chapman; □, △, ○, present MCDS results for $s = 1$, 0.647 and 0.5 respectively; ☆, the present result for helium under wind-tunnel conditions.

predictions for the same gas. The comparison between MCDS and Burnett predictions is also shown in figure 3 for a hard-sphere gas; note that the MCDS predictions do not support the Navier–Stokes results for $s = 0.5$ but do agree with the Burnett results. Thus, the Burnett shock thickness predictions for Mach numbers greater than 1.2 are more accurate than the Navier–Stokes predictions for both hard-sphere and Maxwell gases.

Predicted shock shapes are shown in figure 4. In this case the form of the potential has little effect on the shapes predicted by the MCDS's. Shock shapes as described by the area ratio Q are rather more susceptible to error than the shock thicknesses, hence the noticeable scatter in figure 4. The MCDS shapes follow the Burnett predictions for $s = 1$ due to Simon & Foch (1977) very closely and are clearly different from the Navier–Stokes shock shape predictions. In the limit of low Mach number, the Burnett and Navier–Stokes Q values are qualitatively different, with the MCDS's unequivocally supporting the Burnett values. This conclusion is consistent with the results of Fiscko & Chapman (1988) at higher Mach numbers. Their MCDS's were for Maxwell molecules with VHS scattering. Their lowest-Mach-number result agrees very well with the Burnett $s = 1$ Q values as indicated by the Fiscko–Chapman point plotted in figure 4.

Another quantity that measures shock wave characteristics is the displacement between temperature and density profiles $\Delta_{T\rho}$. The predicted values of $\Delta_{T\rho}$ for Maxwell as well as hard-sphere molecules are shown in figure 5 compared to the

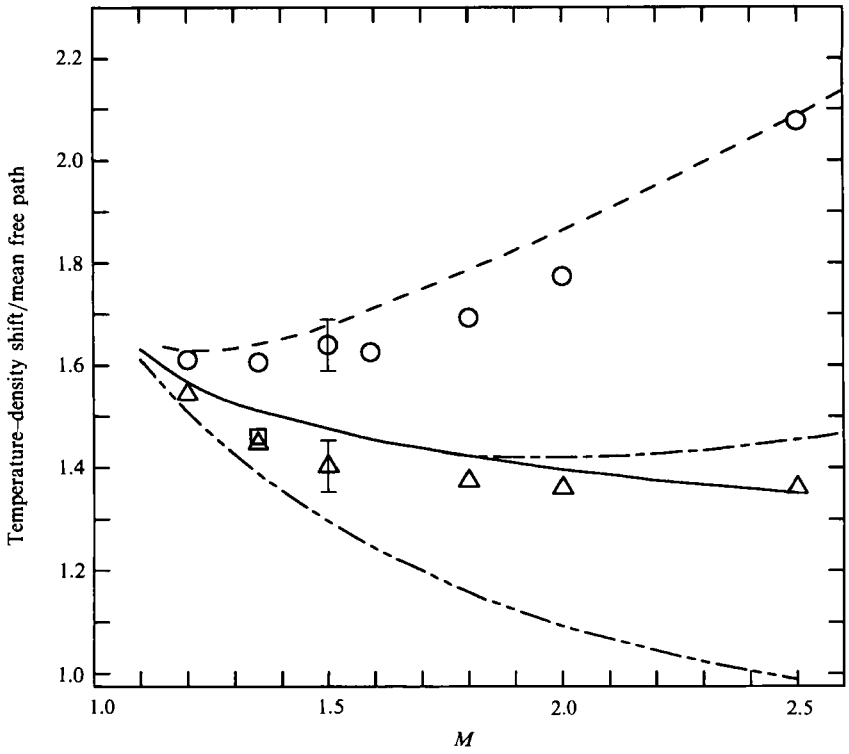

FIGURE 5. Temperature–density shifts: – – –, — · — · —, the $s = 1$ results of Simon & Foch using the Burnett and Navier–Stokes solutions respectively; ——, — · · —, the $s = 0.5$ results of Lumpkin & Chapman using Burnett and Navier–Stokes solutions respectively; ○, △, □, the present MCDS results for $s = 1$, 0.5 and 0.5 (double-precision) respectively.

continuum theories for $s = 1$ and $s = 0.5$ (Lumpkin & Chapman 1991). At very low Mach numbers the scatter of the predictions makes it difficult to assess which theory is more accurate; this precludes drawing any conclusions. However, it may be noted from figure 5 that the MCDS data agree better with the Burnett predictions for Mach numbers greater than approximately 1.3.

Evidence from other phenomena, such as sound propagation, is available (Foch & Ford 1970) and leads to the conclusion that the Burnett equations indeed do offer a better description than the Navier–Stokes equations, even for the conditions encountered in very low-Mach-number shock waves. Measurements of the molecular velocity distribution function in a $M = 1.59$ shock wave by Muntz & Harnett (1969) have been analysed by Holtz, Muntz & Yen (1971). The measurements indicate that the Chapman–Enskog first-iterate predictions of the distribution functions fail for ratios of the local shear stress to pressure $\tau/p \gtrsim 0.05$. The maximum value of τ/p in a $M = 1.3$ monatomic shock is approximately 0.05.

The validity of the Chapman–Enskog procedure has been studied by Elliott (1975). It remains theoretically unclear why the second iterate in that procedure (Burnett equations) is quantitatively more successful than the first iterate (Navier–Stokes equations), although the evidence is now quite strong that this is the case.

4. Conclusions

Based on a previous detailed experimental validation of MCDS, numerical experiments were performed to investigate the adequacy of continuum formulations for non-equilibrium flows of monatomic gases in very low-Mach-number shock waves. It is found that for Mach numbers below about 1.2, shock thicknesses and temperature–density shifts are described to within the MCDS computational scatter by either the Navier–Stokes or the Burnett equations; for Mach numbers greater than 1.2 the Burnett predictions are more accurate. It was also found that shock shapes appear to be far more accurately described by the Burnett predictions for all Mach numbers down to one.

This work was supported in part by NASA/DOD grant NAGW-1061. Forrest Lumpkin and Dean Chapman kindly provided results of their work prior to its publication.

REFERENCES

Aziz, R. A. & Chen, H. H. 1977 An accurate intermolecular potential for argon. *J. Chem. Phys.* **67**, 5719–5726.

Aziz, R. A. & Nain, V. P. S. 1979 An accurate intermolecular potential for helium. *J. Chem. Phys.* **70**, 4336–4341.

Bird, G. A. 1976 *Molecular Gas Dynamics.* Clarendon.

Bird, G. A. 1981 Monte-Carlo simulation in an engineering context. In *Rarefied Gas Dynamics: Proc. 12th Intl Symp.* (ed. S. Fisher), pp. 239–255. AIAA.

Bird, G. A. 1983 Definition of mean free path for real gases. *Phys. Fluids* **26**, 3222–3223.

Bird, G. A. 1989 The perception of numerical methods in rarefied gas dynamics. In *Rarefied Gas Dynamics: Proc. 16th Intl Symp. III: Theoretical and Computational Techniques* (ed. E. P. Muntz, D. Weaver & D. Campbell), pp. 211–226. AIAA.

Chapman, S. & Cowling, T. G. 1952 *The Mathematical Theory of Non-Uniform Gases* (2nd Edn). Cambridge University Press.

Elliott, J. P. 1975 On the validity of the Navier–Stokes relation in a shock wave. *Can. J. Phys.* **53**, 583–586.

Erwin, D. A., Pham-Van-Diep, G. C. & Muntz, E. P. 1991 Nonequilibrium gas flows I: A detailed validation of Monte Carlo direct simulation for monatomic gases. *Phys. Fluids* A **3**, 697–705.

Fiscko, K. A. & Chapman, D. R. 1988 Comparison of shock structure solution using independent continuum and kinetic theory approaches. *SPIE Symp. Innovative Sci. and Technol.*

Fiszdon, W., Herczyński, R. & Walenta, Z. 1974 The structure of a plane shock wave of a monatomic gas. In *Rarefied Gas Dynamics: Proc. 9th Intl Symp.* (ed. M. Becker & M. Fiebig), pp. 23-1–23-57. DFVLR.

Foch, J. D. & Ford, G. W. 1970 The dispersion of sound in monoatomic gases. In *Studies in Statistical Mechanics, vol. V* (ed. J. de Boer & G. E. Uhlenbeck). North-Holland.

Gilbarg, D. & Paolucci, D. 1953 *Arch. Rat. Mech. Anal.* **2**, 617.

Holtz, T., Muntz, E. P. & Yen, S.-M. 1971 Comparison of measured and predicted velocity distribution function in a shock wave. *Phys. Fluids* **14**, 545–548.

Liepmann, H. W., Narasimha, R. & Chahine, M. T. 1962 Structure of a plane shock layer. *Phys. Fluids* **5**, 1313.

Lumpkin, F. & Chapman, D. 1991 Accuracy of the Burnett equations for hypersonic real gas flows. *AIAA Paper* 91-0771.

Muntz, E. P. & Harnett, L. N. 1969 Molecular velocity distribution function measurements in a normal shock wave. *Phys. Fluids* **12**, 2027.

MUNTZ, E. P., PHAM-VAN-DIEP, G. & ERWIN, D. A. 1991 A review of the kinetic detail required for accurate predictions of normal shock waves. In *Rarefied Gas Dynamics: Proc. 17th Intl Symp.* (ed. A. E. Beylich), pp. 198–206. VCH.

PHAM-VAN-DIEP, G. C., ERWIN, D. A. & MUNTZ, E. P. 1989 Highly non-equilibrium molecular motion in a hypersonic shock wave. *Science* **245**, 624–626.

SCHMIDT, B. 1969 Electron beam density measurements in shock waves in argon. *J. Fluid Mech.* **39**, 361–373.

SIMON, C. E. & FOCH, J. D. 1977 Numerical integration of the Burnett equations for shock structure in a Maxwell gas. In *Rarefied Gas Dynamics: Proc. 10th Intl Symp.* (ed J. L. Potter), pp. 493–500. AIAA.

TALBOT, L. & SHERMAN, F. S. 1960 Experiment versus kinetic theory for rarefied gases. In *Rarefied Gas Dynamics: Proc. 1st Intl Symp.* (ed. F. M. Devienne). Pergamon.